# Deficiency of molecular hydrogen in the disk of β Pictoris

**A. Lecavelier des Etangs*, A. Vidal-Madjar*, A. Roberge†, P. D. Feldman†, M. Deleuil‡, M. André†, W. P. Blair†, J.-C. Bouret‡, J.-M. Désert*, R. Ferlet*, S. Friedman†, G. Hébrard*, M. Lemoine* & H. W. Moos†**

* *Institut d'Astrophysique de Paris, CNRS, 98 bis bld Arago, F-75014 Paris, France*
† *Department of Physics and Astronomy, Johns Hopkins University, Baltimore, Maryland 21218, USA*
‡ *Laboratoire d'Astrophysique de Marseille, BP 8, F-13376 Marseille Cedex 12, France*

**Molecular hydrogen ($H_2$) is by far the most abundant material from which stars, protoplanetary disks and giant planets form, but it is difficult to detect directly. Infrared emission lines from $H_2$ have recently been reported[1] towards β Pictoris, a star harbouring a young planetary system[2]. This star is surrounded by a dusty 'debris disk' that is continuously replenished either by collisions between asteroidal objects[3] or by evaporation of ices on Chiron-like objects[4]. A gaseous disk has also been inferred from absorption lines in the stellar spectrum[5–8]. Here we present the far-ultraviolet spectrum of β Pictoris, in which $H_2$ absorption lines are not seen. This allows us to set a very low upper limit on the column density of $H_2$: $N(H_2) \leq 10^{18}\,cm^{-2}$. This non-detection is puzzling when compared to the quantity of $H_2$ inferred from the infrared observations, but it does show that $H_2$ is not in the disk on the direct line of sight. Carbon monoxide (CO) has been seen in absorption against the star[8–10], yielding a ratio of $CO/H_2 > 6\times10^{-4}$. As CO would be destroyed under ambient conditions in about 200 years (refs 9, 11), our result demonstrates that the CO in the disk arises from evaporation of planetesimals.**

The age of β Pic (about 20 Myr; ref. 12) indicates that the planetary system around this star is likely to be in the late stage of formation—the clearing of the remaining planetesimals. An extensive spectroscopic survey has revealed very rapid spectral variations, interpreted as hundreds of star-grazing comets passing in front of the star[13,14]. The gas component also shows the presence of CO, seen in ultraviolet (UV) absorption lines[8–10].

Observation of far-UV electronic transitions is the most powerful tool for detection of cold molecular hydrogen. Although very abundant, this symmetric molecule does not radiate at radio wavelengths, and thus remained undetected until its absorption signatures from Werner and Lyman series were detected by space missions, such as the Copernicus satellite in the early 1970s[15–17]. As absorption lines of CO were easily detected towards β Pic, it was expected that $H_2$ would be detected by the Far Ultraviolet Spectroscopic Explorer (FUSE)[18] satellite. Moreover, a large quantity of $H_2$ has recently been inferred to exist in the β Pic system, on the basis of detection by the ISO satellite of its infrared emission lines[1]. If this $H_2$ is co-spatial with the dust, it should be readily detectable by far-UV spectroscopy of the star seen through its edge-on disk.

FUSE observations of β Pic were made on 18 March 2000 with a test exposure of 5,800 s, and on 1 and 3 March 2001 for a total time of about 28,800 s. This star is very faint in the far-UV, and hence its continuum is almost undetectable at the wavelengths of the $H_2$ transitions (Fig. 1): in the 1,108-Å region where we could expect to see the $H_2$ (0–0) band in absorption, the signal-to-noise ratio is less than 1 per 0.1 Å. However, the clear presence of the stellar O VI emission doublet at 1,031.9 and 1,037.6 Å, and the faint emission from C II at 1,036.3 Å, provide the opportunity to strongly constrain the $H_2$ content along the line of sight. With rest wavelengths of 1,036.55 Å ($J = 0$), 1,037.15 Å and 1,038.16 Å ($J = 1$), and 1,038.69 Å ($J = 2$), the $H_2$ (5–0) lines are exactly superimposed on the weaker line of the O VI doublet. The $H_2$ lines at $J = 3$ (1,031.20 Å) and $J = 4$ (1,032.35 Å) are superimposed on the stronger line of the doublet.

The O VI emission lines that we detect cannot originate in the interstellar medium, nor can they be scattered solar light. Indeed, the interstellar diffuse emission is 100 times fainter and, furthermore, simultaneous spectra acquired with the MDRS (medium resolution) aperture of FUSE, pointed about 200 arcsec away from β Pic, do not show any emission other than airglow lines. These O VI lines thus originate from β Pic[19], and allow us to probe the line of sight towards the star through the edge-on circumstellar disk.

If $H_2$ were present in substantial quantity in the line of sight, the O VI line at 1,038 Å would be absorbed, and hence would appear abnormally weak—less than half the intensity of the other O VI line at 1,032 Å (Fig. 2). For instance, in the spectrum of the Herbig Ae star AB Aurigae, the O VI line at 1,038 Å is almost totally absorbed and a corresponding $H_2$ column density of $7\times10^{19}\,cm^{-2}$ has been derived[20]. In β Pic, emission is seen in both lines of the O VI doublet with an integrated flux ratio close to the expected value of 2. This implies that $H_2$ is not present in a quantity sufficient to significantly absorb the O VI emission around 1,038 Å. We have detected more than 6,000 photons in the O VI line, compared to 3,000 photons due to the background noise; $H_2$ column density above a few times $10^{20}\,cm^{-2}$ is thus excluded at the $\sim45\sigma$ level.

A better upper limit on the amount of $H_2$ can be estimated by assuming the intrinsic width of the $H_2$ lines to be very small. The absence of wide absorption lines thus gives a conservative upper

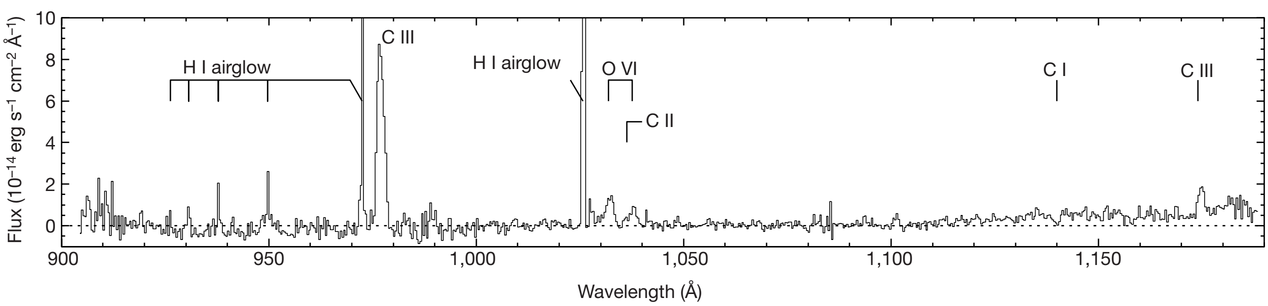


**Figure 1** Far ultraviolet spectrum of β Pic from 905 to 1,188 Å, as obtained by the FUSE satellite. The target was acquired in the LWRS (low resolution) slit of 30″ × 30″ after a blind offset from a reference star. The data have been processed with the 'calfuse' pipeline software, version 1.8.7. The atmospheric H I airglow lines of the Lyman series are detected from Lyβ (1,025.7 Å) to Lyη (926.2 Å). We also detect the stellar continuum down to ~1,100 Å. This continuum is well reproduced by a Kurucz model with an effective temperature of 8,200 K, a turbulent velocity of 2 km s$^{-1}$, and surface gravity log $g$ = 4.25. C I photospheric lines predicted by the stellar model are seen near 1,140 Å. From the position of a few stellar photospheric lines, the uncertainty in the wavelength calibration is less than 40 km s$^{-1}$. C II, C III and O VI are also detected in emission.

limit on the column density of $H_2$, which corresponds to the limit at which the 'wings' of saturated absorption lines in the lorentzian part of the profile would start to become detectable.

We may have marginally detected an absorption line of $H_2$ at $J = 0$. We infer a corresponding column density $N_{J=0}$ of $8 \times 10^{17}\,\mathrm{cm}^{-2}$, assuming that the emission line is smooth in this wavelength region. However, because the line is located between the C II and O VI emission lines, this 'detection' could be an artefact arising from the lack of emission precisely at this wavelength. In any case, the absence of a wide absorption line allows us to constrain the column density of $H_2$ at $J = 0$. A column density $N_{J=0} = 3 \times 10^{18}\,\mathrm{cm}^{-2}$ increases the $\chi^2$ of the fit to the data by 4 in comparison to the fit of the emission lines without $H_2$. We conclude that the column density of $H_2$ at $J = 0$ is below $3 \times 10^{18}\,\mathrm{cm}^{-2}$ at the 95% confidence level.

The column densities of $H_2$ at $J = 1$ to $J = 4$ are better constrained, because they are well superimposed on the O VI lines. We find the following upper limits at the 95% confidence level: $N_{J=1} \leq 5 \times 10^{17}\,\mathrm{cm}^{-2}$, $N_{J=2} \leq 8 \times 10^{17}\,\mathrm{cm}^{-2}$, $N_{J=3} \leq 4 \times 10^{17}\,\mathrm{cm}^{-2}$ and $N_{J=4} \leq 1 \times 10^{17}\,\mathrm{cm}^{-2}$. The upper limit for $N_{J=0}$ is slightly less well constrained. However, the probability that $N_{J=0}$ is larger than $N_{J=1}$ is low; this would require a temperature lower than 20 K at thermodynamic equilibrium. With the assumption that $N_{J=0} \leq N_{J=1}$, we obtain an upper limit for the total $H_2$ column density toward β Pic: $N(H_2) \leq 10^{18}\,\mathrm{cm}^{-2}$ at the 95% confidence level (Fig. 2).

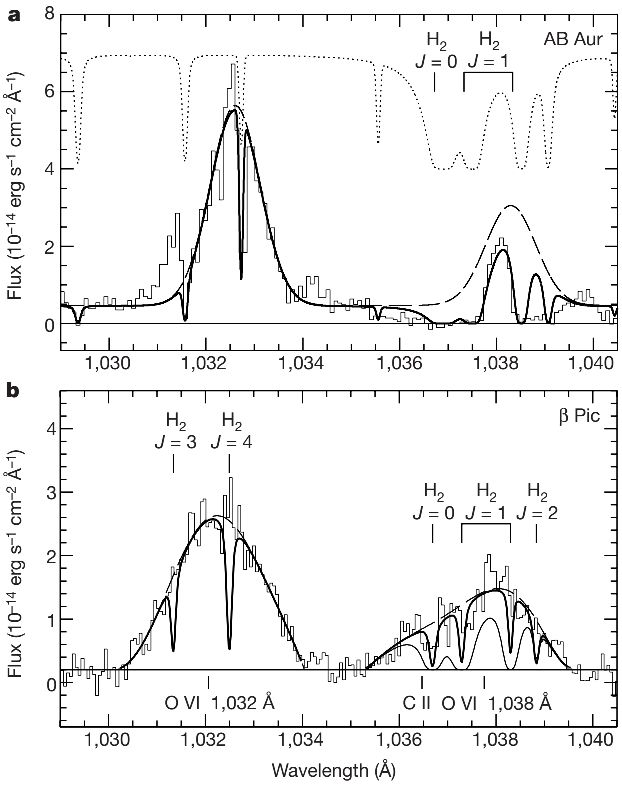


**Figure 2** Plot of the observed O VI emission doublet and $H_2$ absorption lines. **a**, For the Herbig star AB Aur[20], the O VI line at 1,032 Å is well fitted by a gaussian (dashed line). The O VI emission line at 1,038 Å is almost completely absorbed by a $H_2$ column density of $N(H_2) = 7 \times 10^{19}\,\mathrm{cm}^{-2}$. The normalized $H_2$ model is shown with a dotted line. Only a small window between the two $J = 1$ lines of $H_2$ allows a fraction of the emission to be seen (solid line). **b**, For β Pic, the wide O VI and C II emission lines are fitted with a polynomial (dashed line). The flux ratio of the two O VI lines is close to the theoretical value of 2, providing a direct indication of the low column density of $H_2$. The thick solid line shows the expected spectrum for a $H_2$ column density of $N(H_2) = 10^{18}\,\mathrm{cm}^{-2}$ in each $J$-level. Except for $J = 0$, such a high column density is excluded at more than the 99% confidence level. The thin solid line shows the modelled spectrum if $H_2$ were present with a total column density of $5 \times 10^{19}\,\mathrm{cm}^{-2}$ and a temperature of 109 K, as given by the ISO observations of the 17- and 28-μm emission lines[1]. At this temperature, 34% of the $H_2$ molecules are at $J = 0$, whereas 64% are at $J = 1$. The total column density of $5 \times 10^{19}\,\mathrm{cm}^{-2}$ is actually only one-tenth of the lowest possible $H_2$ column density indicated by the ISO observations, if the $H_2$ were co-spatial with the dust. Such a model is rejected at more than $\sim 20\sigma$. If the $H_2$ detected by ISO were uniformly distributed in the disk, the O VI emission line at 1,038 Å would be completely absorbed and rendered undetectable in the present observation.

This upper limit on the $H_2$ column density obtained from the FUSE spectrum is very low, which has several consequences. First, the CO detected in UV spectra of β Pic (obtained by the Hubble Space Telescope) has a column density $N(CO)$ of $6 \times 10^{14}\,\mathrm{cm}^{-2}$ (ref. 8). Without any geometrical assumptions, we find $N(CO)/N(H_2) > 6 \times 10^{-4}$. This ratio towards β Pic is two orders of magnitude higher than the value for interstellar translucent clouds having a similarly low column density of CO (ref. 21). This proves that the CO is not interstellar, but is instead located in the disk. However, the published modelling of the β Pic CO abundance—which assumes chemical equilibrium within a dense molecular circumstellar disk—predicts a $H_2$ column density of the order of $10^{22}\,\mathrm{cm}^{-2}$ (ref. 22), in disagreement with the present observation. Such a high column density is required to shield CO from dissociation by interstellar UV photons, and thus to allow the formation of CO. The present result shows that the gaseous disk has a low density, and that CO cannot form by the same chemical reaction that produces interstellar CO. On the contrary, at the estimated low column density of $H_2$, photodissociation dominates, destroying CO on a timescale of about 200 years (refs 9, 11). This implies that CO must be re-supplied to the circumstellar disk by release from a pre-existing reservoir. Two processes have been proposed: either evaporation of star-grazing comets, or a slow evaporation of planetesimals on moderately eccentric orbits at several tens of astronomical units (AU) from the star, as observed for Chiron in the Solar System[23]. The evaporation naturally explains the large $CO/H_2$ ratio: CO is trapped in the ices sublimed from the evaporating bodies, whereas $H_2$ cannot be trapped in this way.

The present $H_2$ upper limit is well below the recently reported $H_2$ detection from ISO observations using the SWS spectrometer[1]. From the two emission lines of $H_2$ at 17 and 28 μm, a total $H_2$ mass of 0.17 Jupiter masses was inferred within the ISO beam (280 AU × 540 AU and 400 AU × 540 AU for the two lines, respectively). If this $H_2$ were distributed like the dust in the edge-on disk, a column density of $5 \times 10^{20}$ to $5 \times 10^{22}\,\mathrm{cm}^{-2}$ should have been detected in absorption, depending on the geometry and inclination of the system. In other words, the present upper limit on the $H_2$ column density constrains the total mass in the disk to be below $\sim 3 \times 10^{-4}$ Jupiter masses. This discrepancy of three orders of magnitude needs to be explained.

ISO has detected $H_2$ only in the high rotational levels $J = 2$ and $J = 3$, which contain less than 2% of the total mass, at a temperature of 109 K determined by the ratio of the two emission lines. FUSE gives access to the $J = 0$ and $J = 1$ levels as well, where most of the $H_2$ is found, at the typical temperatures of the interstellar medium or circumstellar disks. The present upper limit for $H_2$ ($J = 2$) implies that the mass of $H_2$ ($J = 2$) in the disk is more than ten times smaller than the mass of $H_2$ ($J = 2$) seen in the infrared.

We therefore conclude that the $H_2$ detected by ISO cannot be uniformly distributed within the disk of β Pic (the opening angle of the dust disk is larger than its inclination). Nor can it be distributed in a single large cloud in front of β Pic: 0.17 Jupiter masses distributed homogeneously across the full ISO beam would yield a $H_2$ column density of the order of $2 \times 10^{21}\,\mathrm{cm}^{-2}$. Any such cloud in the foreground of β Pic would have been readily detected. The possibility that ISO detected an interstellar molecular cloud beyond β Pic is also excluded, because the non-detection of CO radio emission in a similar beam would imply a very abnormal $CO/H_2$ ratio[24]. Finally, we note that, because the O VI emission lines are more than 2 Å wide, only $H_2$ gas Doppler-shifted by more than

600 km $s^{-1}$ could escape detection; this is unlikely, as 600 km $s^{-1}$ is greater than the escape velocity. Consequently, neither *J*-level population ($J = 2$ is not detected) nor Doppler shift can explain the discrepancy. If the $H_2$ seen in the infrared were located in the disk, it would have been detected in our FUSE observation.

A solution to this problem is to consider that $H_2$ is not distributed widely throughout the disk. If the ISO detection is confirmed by further observations, we suggest that the $H_2$ could be confined into individual clouds, none of which intersected the small volume of the β Pic line of sight at the time of our FUSE observations. Such $H_2$ clouds would easily escape detection in absorption, but would be seen in emission. The nature of these clouds remains unclear; however, we speculate that they might be remnants of gaseous planet embryos which captured a significant amount of protoplanetary material before its recent dissipation. The stability, number and density of these putative clouds need to be analysed. Given that 0.17 Jupiter masses is a huge amount of gas, these clouds should have large physical sizes and/or be relatively numerous. The discrepancy between the ISO detection and the present negative FUSE result remains a challenging issue.

Using ISO, even larger amounts of $H_2$ have been reported[1] for other similar, albeit younger, circumstellar disks. Again the nature and the geometrical distribution of this $H_2$ remain to be determined. The present result shows that, in the circumstellar disks, dust is not a good indicator of the $H_2$ distribution; it also shows that CO may not generally be as depleted in the disks as may be concluded simply from the observed ratio of CO and $H_2$ emission. On the contrary, CO could be over-abundant compared to the standard $CO/H_2$ ratio; this provides a clue to the evaporation activity related to large-scale motions of the remnant planetesimals being cleared from the young planetary disk. □

Received 14 March; accepted 12 June 2001.

1. Thi, W. F. *et al.* Substantial reservoirs of molecular hydrogen in the debris disks around young stars. *Nature* **409,** 60–63 (2001).
2. Vidal-Madjar, A., Lecavelier des Etangs, A. & Ferlet, R. Beta Pictoris, a young planetary system? A review. *Planet. Space Sci.* **46,** 629–648 (1998).
3. Backman, D. E. & Paresce, F. Main-sequence stars with circumstellar solid material—The Vega phenomenon. *Protostars and Planets III* (eds Levy, E. H. & Lunine, J. I.) 1253–1304 (Univ. Arizona Press, 1993).
4. Lecavelier des Etangs, A., Vidal-Madjar, A. & Ferlet, R. Dust distribution in disks supplied by small bodies: is the Beta Pictoris disk a gigantic multi-cometary tail? *Astron. Astrophys.* **307,** 542–550 (1996).
5. Hobbs, L. M., Vidal-Madjar, A., Ferlet, R., Albert, C. E. & Gry, C. The gaseous component of the disk around Beta Pictoris. *Astrophys. J.* **293,** L29–L33 (1985).
6. Vidal-Madjar, A., Ferlet, R., Hobbs, L. M., Gry, C. & Albert, C. E. The circumstellar gas cloud around Beta Pictoris. II. *Astron. Astrophys.* **167,** 325–332 (1986).
7. Lagrange, A.-M. *et al.* The Beta Pictoris circumstellar disk. XXIV. Clues to the origin of the stable gas. *Astron. Astrophys.* **330,** 1091–1108 (1998).
8. Roberge, A. *et al.* High-resolution Hubble Space Telescope STIS spectra of CI and CO in the Beta Pictoris circumstellar disk. *Astrophys. J.* **538,** 904–910 (2000).
9. Vidal-Madjar, A. *et al.* HST-GHRS observations of Beta Pictoris: additional evidence for infalling comets. *Astron. Astrophys.* **290,** 245–258 (1994).
10. Jolly, A. *et al.* HST - GHRS observations of CO and CI in the Beta Pictoris circumstellar disk. *Astron. Astrophys.* **329,** 1028–1034 (1998).
11. van Dishoeck, E. F. & Black, J. H. The photodissociation and chemistry of interstellar CO. *Astrophys. J.* **334,** 771–802 (1988).
12. Barrado y Navascués, D., Stauffer, J. R., Song, I. & Caillault, J.-P. The age of Beta Pictoris. *Astrophys. J.* **520,** L123–L126 (1999).
13. Ferlet, R., Vidal-Madjar, A. & Hobbs, L. M. The Beta Pictoris circumstellar disk. V- Time variations of the CA II-K line. *Astron. Astrophys.* **185,** 267–270 (1987).
14. Beust, H., Vidal-Madjar, A., Ferlet, R. & Lagrange-Henri, A. M. The Beta Pictoris circumstellar disk. X-Numerical simulations of infalling evaporating bodies. *Astron. Astrophys.* **236,** 202–216 (1990).
15. Carruthers, G. R. Rocket observation of interstellar molecular hydrogen. *Astrophys. J.* **161,** L81–L85 (1970).
16. Spitzer, L. *et al.* Spectrophotometric results from the Copernicus satellite. IV. Molecular hydrogen in interstellar space. *Astrophys. J.* **181,** L116–L121 (1973).
17. Shull, J. M. & Beckwith, S. Interstellar molecular hydrogen. *Annu. Rev. Astron. Astrophys.* **20,** 163–190 (1982).
18. Moos, H. W. *et al.* Overview of the Far Ultraviolet Spectroscopic Explorer Mission. *Astrophys. J.* **538,** L1–L6 (2000).
19. Deleuil, M. *et al.* Is Beta Pictoris an active star? *Astrophys. J.* (in the press).
20. Roberge, A. *et al.* FUSE and HST STIS observations of hot and cold gas in the AB Aurigae system. *Astrophys. J.* **551,** L97–L100 (2001).
21. Magnani, L., Onello, J. S., Adams, N. G., Hartmann, D. & Thaddeus, P. The variation of the CO to $H_2$ conversion factor in two translucent clouds. *Astrophys. J.* **504,** 290–299 (1998).
22. Kamp, I. & Bertoldi, F. CO in the circumstellar disks of Vega and Beta Pictoris. *Astron. Astrophys.* **353,** 276–286 (2000).
23. Lecavelier des Etangs, A. Circumstellar disks and outer planet formation. *Planets Outside the Solar System: Theory and Observations* (eds Mariotti, J.-M. & Alloin, D.) 95–103 (Kluwer Academic, Dordrecht/Boston, 1999).
24. Liseau, R. & Artymowicz, P. High sensitivity search for molecular gas in the Beta Pic disk. On the low gas-to-dust mass ratio of the circumstellar disk around Beta Pictoris. *Astron. Astrophys.* **334,** 935–942 (1998).

**Acknowledgements**

We thank Gopal-Krishna, G. Pineau des Forêts and S. Cabrit for discussions, and R. Kurucz for providing a model of the β Pic stellar atmosphere. The work at Johns Hopkins University was supported by NASA; the work at the Institut d'Astrophysique de Paris and at LAM was supported by CNES. The work reported here is based on data obtained by the NASA-CNES-CSA FUSE mission, operated by the Johns Hopkins University.

Correspondence and requests for materials should be addressed to A.L.d.E. (e-mail: lecaveli@iap.fr).

# Origin of the Moon in a giant impact near the end of the Earth's formation

**Robin M. Canup* & Erik Asphaug†**

* *Department of Space Studies, Southwest Research Institute, 1050 Walnut Street, Suite 426, Boulder, Colorado 80302, USA*
† *Department of Earth Sciences, University of California, Santa Cruz, California 95064, USA*

**The Moon is generally believed to have formed from debris ejected by a large off-centre collision with the early Earth[1,2]. The impact orientation and size are constrained by the angular momentum contained in both the Earth's spin and the Moon's orbit, a quantity that has been nearly conserved over the past 4.5 billion years. Simulations of potential moon-forming impacts now achieve resolutions sufficient to study the production of bound debris. However, identifying impacts capable of yielding the Earth–Moon system has proved difficult[3–6]. Previous works[4,5] found that forming the Moon with an appropriate impact angular momentum required the impact to occur when the Earth was only about half formed, a more restrictive and problematic model than that originally envisaged. Here we report a class of impacts that yield an iron-poor Moon, as well as the current masses and angular momentum of the Earth–Moon system. This class of impacts involves a smaller—and thus more likely—object than previously considered viable, and suggests that the Moon formed near the very end of Earth's accumulation.**

The strength of the impact hypothesis over alternative models rests on its ability to account for (1) the initial ~5-hour terrestrial day implied by the Earth–Moon system angular momentum ($L_{E\text{–}M} = 3.5 \times 10^{41}$ g cm$^2$ s$^{-1}$); and (2) the ejection of sufficient iron-depleted material into orbit to yield the Moon, which has an unusually small metallic core comprising $\lesssim$3% of its mass[7]. Many works[3–5,8–12] have modelled potential moon-forming impacts, most using a method known as smooth particle hydrodynamics, or SPH[13]. In SPH, objects are evolved in time by estimating their state and dynamical variables at discrete points that are smoothed over spherical overlapping kernel functions. This lagrangian technique requires no underlying grid, and is well suited to intensely deforming systems evolving within mostly empty space.

Recent SPH simulations[4,5] identify two classes of impacts capable of placing sufficient mass into orbit to yield the Moon, but neither is entirely satisfactory. The first involves impacts with angular

  